International Journal of Pharmaceutics, 95 (1993) 143–151

IJP 03185

Dissolution studies of hexamethylmelamine

Gordon A. Rodley [1], Hak-Kim Chan [2] and Igor Gonda [2]

Department of Pharmacy, University of Sydney, Sydney, NSW 2006 (Australia)

(Received 14 April 1992)
(Modified version received 14 December 1992)
(Accepted 7 January 1993)

Key words: Crystal habit; Dissolution; Hexamethylmelamine; Activation energy; Anisotropy; Orientational factor

Summary

A study has been made of the dissolution rates of 'end' and 'side' faces of single crystals of the anti-tumour drug hexamethylmelamine (HMM). The results demonstrate preferential dissolution of the end faces. Various features of the dissolution process show that it is surface-reaction rather than diffusion controlled. Comparisons are made with results from an earlier study of the growth of HMM crystals. It is concluded that geometrical features of the crystal packing of HMM molecules play a rate-determining role in the dissolution process.

Introduction

The intrinsic rate of dissolution of pharmaceutical crystals is determined by the energetics (including defects) and external morphology (or 'habit') of the crystals (Burt and Mitchell, 1980, 1981; Chan and Grant, 1989). Dissolution anisotropy for individual crystal habits can result from different surface reactions on different crystal faces. This effect has been studied in some detail using single crystals of an inorganic compound (Burt and Mitchell, 1979).

We have carried out extensive studies on the crystal growth of an anti-tumour drug hexamethylmelamine (HMM) (Aroney et al., 1987; Chan et al., 1990, 1991). The most notable general feature is the formation of a 'needle' habit from polar solvents and a 'compact' form from non-polar solvents.

This study was carried out in order to see if similar differences between solvents, and between different faces of single crystals, could be measured during dissolution when bulk diffusion is not rate-determining.

Experimental

Crystals of HMM of length about 1–2 mm were individually placed at the centre of a glass Petri dish of 10 cm diameter and covered with 35

Correspondence to: I. Gonda, Genentech Inc., 460 Point San Bruno Boulevard, South San Francisco, CA 94080, U.S.A.
[1] *Present address:* Centre for Cellular and Molecular Biology, Hyderabad, India.
[2] *Present address:* Genentech Inc., 460 Point San Bruno Boulevard, South San Francisco, CA 94080, U.S.A.

ml of solvent. During the time course of the measurement, the amounts of HMM dissolved were estimated from the change in the dimensions of the crystals (1 mm for length, 0.5 mm for width; density of HMM crystals 1.11 g/cm^3) to be less than 0.5 mg. The latter corresponds to less than 1/100 of the saturation level of the solute in methanol (23.1 mg/ml) and in cyclohexane (38.7 mg/ml) at 25°C. Thus, sink conditions were maintained during dissolution. Two different methods of stirring were employed. In one case the solvent was 'stirred' by passing it through a peristaltic pump with the inlet and outlet tubes (internal bore of 0.5 mm) placed in opposite directions at one point on the circumference of the Petri dish so that a circular motion of the solvent was produced. The pump was run at rates between 25–70 ml/min. In the second method a

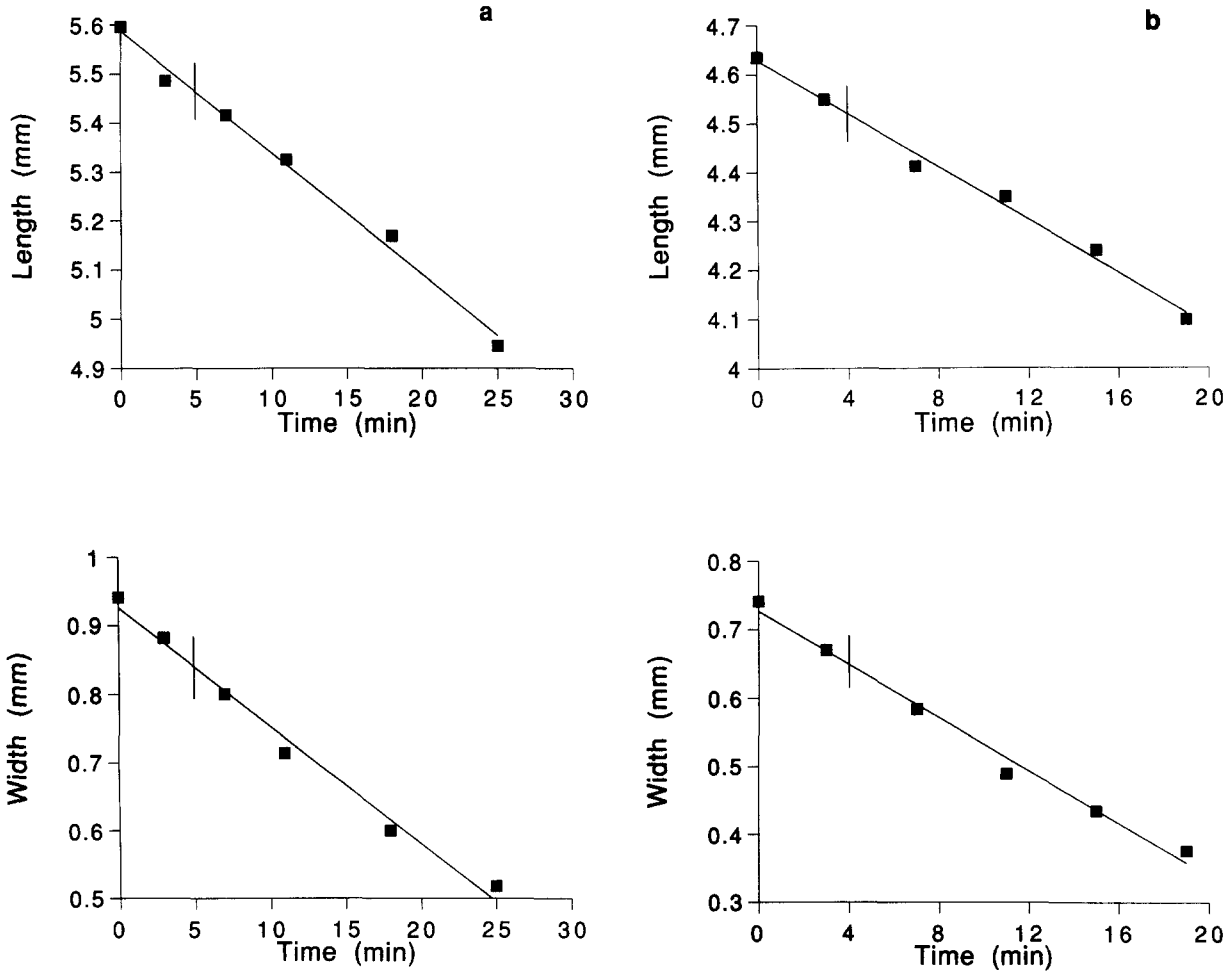

Fig. 1. Changes in lengths and widths (in mm) of crystals with time (in min): (a) run 7 and (b) run 8. The vertical lines show the times of commencement of stirring.

small magnetic stirrer (approx. 4×1.5 mm) was used to agitate the solution.

The Petri dish was covered and enclosed in a polystyrene 'thermal' box in order to maintain the temperature within ± 1°C of a particular value. In low temperature studies ice or solid CO_2 were placed inside the box. For isothermal studies the temperature was measured by a thermometer placed in the box. For studies at two different temperatures (in activation energy studies) a thermistor was placed directly into the solvent.

In some of the studies the crystals were kept in a fixed position in the Petri dish by adhesive material (Blu-tack, Emhart Australia, Vic., Australia). In other cases the crystals were located on the end on a small holder in order to raise them from the bottom surface of the Petri dish. The crystal was generally illuminated from underneath the Petri dish. The image of the crystal was recorded by a video camera with a focal length of 5 cm, digitised and stored on an image analysis system (Imageplus +, Dapple Systems, Sunnyvale, CA) for subsequent analysis. The image of the crystal was focussed so that the edges were visible as sharply as possible. The same focus was maintained throughout the runs. This generally enabled a reasonably clear image to be obtained at all times. The images taken at particular inter-

TABLE 1

Dissolution data

Sample no.	Temperature (K) [a]	Length (mm)	Width (mm)	Length/ width	Crystal type [b]	Solvent [c]	Stirring [d]	R_L ($\times 10^2$) (mm min^{-1})	R_W ($\times 10^2$) (mm min^{-1})	R_L/R_W
1	301.5	3.2370	0.8580	3.77	1	1	1	1.796	1.753	1.025
2	300.5	4.7970	0.7800	6.15	1	1	1	5.490	3.529	1.556
3	302.0	5.5380	1.0920	5.07	1	1	1	6.086	3.310	1.839
4	297.5	2.2113	1.4391	1.54	0	2	1	4.078	2.400	1.699
5	298.5	4.2900	0.6630	6.47	1	1	0	2.561	2.024	1.265
6	300.5	7.1370	0.7800	9.15	1	1	1	3.922	2.208	1.776
7	298.5	5.5960	0.9360	5.83	1	1	1	2.482	1.714	1.449
8	299.0	4.6020	0.7410	6.21	1	1	1	2.722	1.937	1.405
9	302.0	5.8110	0.5070	11.46	1	1	1	4.314	2.459	1.754
10	295.0	8.3070	0.6242	13.31	1	2	0	2.631	1.016	2.591
11	297.5	5.8500	0.8580	6.82	1	3	0	2.090	0.941	2.221
12	298.0	2.7300	1.1310	2.41	0	1	1	3.667	1.816	2.019
13	271.0	6.7860	0.8190	8.29	1	1	0	1.043	0.549	1.900
14	288.5	6.0840	0.6240	9.75	1	1	0	3.984	2.192	1.818
15	298.0	3.1746	1.1076	2.87	0	2	0	3.216	2.431	1.323
16	290.0	1.5951	0.6903	2.31	0	1	0	2.988	1.624	1.841
17	290.5	3.0030	1.7160	1.75	0	1	1	1.992	1.396	1.427
18	288.5	2.3400	1.4040	1.67	0	1	1	1.961	1.376	1.424
19	289.0	2.1840	0.9360	2.33	0	1	1	1.427	0.961	1.486
20	289.5	3.3150	1.1076	2.99	0	1	0	2.667	1.686	1.581
21	290.0	1.7043	0.6942	2.46	0	2	0	3.961	2.212	1.791
22	290.0	1.1700	0.9321	1.26	0	2	0	1.118	0.678	1.647
23	293.0	2.7573	1.1544	2.39	0	1	0	1.671	1.012	1.651
24	290.5	1.7277	0.6357	2.72	0	1	0	1.706	1.306	1.306
25	291.0	2.5077	0.8658	2.90	0	1	0	2.667	1.451	1.838
26	291.5	3.3813	1.0647	3.18	0	1	0	1.914	1.875	1.021
27	291.0	4.4460	1.4118	3.15	0	1	0	1.875	1.396	1.343
28	263.0	3.2370	0.8892	3.64	1	1	0	0.710	0.506	1.403
29	276.5	2.8860	0.7566	3.81	1	1	0	1.435	1.094	1.312
30	291.0	3.2760	1.1037	2.97	0	1	0	3.208	2.624	1.223
31	291.5	4.2900	0.8775	4.84	1	1	0	2.549	2.451	1.040

TABLE 1 (continued)

Sample no.	Temperature (K) [a]	Length (mm)	Width (mm)	Length/ width	Crystal type [b]	Solvent [c]	Stirring [d]	R_L ($\times 10^2$) (mm min^{-1})	R_W ($\times 10^2$) (mm min^{-1})	R_L/R_W
32	280.0	3.9000	0.4758	8.20	1	1	0	1.882	1.490	1.263
33	277.5	3.1590	0.7722	4.10	1	1	0	1.522	1.176	1.293
34	289.0	2.8860	0.4212	6.85	1	1	0	2.745	2.188	1.254
35	300.5	2.1060	0.5928	3.55	1	1	0	8.078	4.392	1.839
36	281.0	1.7550	0.3471	5.06	1	1	0	1.718	1.227	1.399
37	289.0	3.5490	0.5499	6.45	1	1	0	1.827	2.059	0.888
38	292.0	3.6270	0.8424	4.31	1	1	0	3.810	2.596	1.471
39	292.0	3.1980	0.7254	4.41	1	1	0	3.349	2.137	1.567
40	263.5	3.2370	0.4407	7.35	1	1	0	1.569	0.686	2.286
41	263.5	2.6130	0.3939	6.63	1	1	0	1.537	0.620	2.481
42	266.5	2.6520	0.6630	4.00	1	1	0	0.870	0.478	1.810
43	293.5	2.4570	0.4407	5.58	1	1	0	3.059	1.553	1.970
44	267.0	3.5100	0.8541	4.11	1	1	0	0.635	0.502	1.266
45	295.5	2.9640	0.6045	4.90	1	1	0	6.604	3.200	2.064
46	294.5	2.9250	0.9243	3.16	0	1	0	4.761	3.251	1.464
47	256.0	2.4570	0.3588	6.85	1	1	0	0.714	0.416	1.717
48	293.0	4.6800	1.0608	4.41	1	1	0	2.682	2.486	1.079
49	255.0	3.9000	0.6357	6.13	1	1	0	0.471	0.235	2.000
50	294.0	1.7550	0.9984	1.76	0	1	0	4.204	2.478	1.696
51	281.0	1.2480	0.6045	2.06	0	1	0	1.969	1.431	1.375
52	294.0	2.9250	0.7566	3.87	1	1	1	3.404	2.984	1.141
53	262.0	2.7300	0.4680	5.83	1	1	1	1.129	1.145	0.986

[a] All temperature measurements within ±1°C except No. 1 (±1.5°C) and No. 20 (±2°C).
[b] L/W > 3.5 designated as '1' = 'needle'. L/W < 3.5 designated as '0' = 'compact'.
[c] 1, methanol; 2, cyclohexane; 3, iso-octane.
[d] 1, stirred run; 0, unstirred run.

vals were analysed for changes in length and width, based on calibration measurements. The crystals were located in a wide range of different orientations in order to minimise the effect of any orientation bias. The image analysis error due to the latter was shown to be not more than about 5%.

The study used methanol as the main solvent, with cyclohexane and cyclooctane also being studied to a limited extent. All solvents were of analytical grade.

In the case of the activation energy studies, the same crystal was used for dissolution measurement at both a low and a high temperature. Also, both low-first and high-first sequences of temperature were studied. These procedures were found necessary because of the widely different dissolution characteristics of crystals, not only from one to another but sometimes also for the same crystal.

As entrapped liquid was observed in some crystals of HMM, a ^{1}H-NMR study was made of powdered and crystalline samples in order to identify whether the liquid was the crystallising solvent (acetone). The powdered sample was that of ground up crystals heated to about 70°C. The crystalline samples were air dried. These samples were dissolved in $CDCl_3$ for the NMR measurements for the presence of acetone. The experiments were carried out on a 90 MHz NMR spectrometer (Jeol FX90Q FT NMR) with a Texas 980B computer using Jeol FT NMR FG/BG software. The operating conditions were: frequency 916 Hz, datapoints 8K and deuterium lock signal for tuning.

Results

Usually at least three measurements were made for each crystal and the rate of dissolution

determined by linear regression (coefficient of determination R^2 (adj) values were typically 97% or higher). The results for stirred runs are presented in Fig. 1. The vertical bars indicate the time of commencement of stirring. The observation that the initial readings generally fall on the linear extrapolation of the stirred portion of the curve indicates that the rates of dissolution are not influenced by diffusional factors. When higher rates of stirring were used, than those employed in the runs shown in Fig. 1, the crystals developed markedly pointed ends (when held at one end). This indicated that at these rates of stirring erosion of the crystals occurred. Thus, the stirring rates need to be high enough to overcome bulk diffusion control but low enough to prevent erosion.

The overall data for R_L (rate of dissolution of the length of the crystal) and R_W (rate of dissolution of the width) values are given in Table 1 and plotted in Fig. 2. The regressional analysis of R_L vs R_W gives a value of 1.57 for R_L/R_W with a coefficient of determination R^2 (adj) value of 83% ($R_L = -0.058 + 1.57R_W$ for the data listed in Table 1, where R_L and R_W are expressed in units of 10^{-2} mm min^{-1}).

Further regressional analyses show that there is no correlation of the dissolution rate values with either the presence or absence of stirring or with size (length, breadth or projected area) of the crystals: R^2 (adj) values ranged from 0.0 to 0.7%, and p values ranged from 0.24 to 0.97.

The limited study of solvents other than methanol indicated that the R_L/R_W value is essentially independent of the nature of the solvent. This is further evidence that the dissolution is not influenced by diffusion, especially as the rates of dissolution were significantly slower (than for methanol) when iso-octane was used.

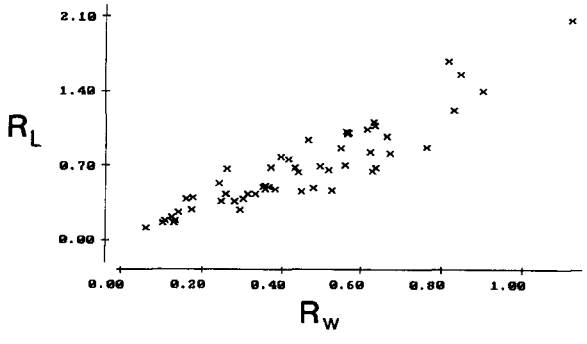

Fig. 2. Plot of R_L vs R_W values for all crystals studied.

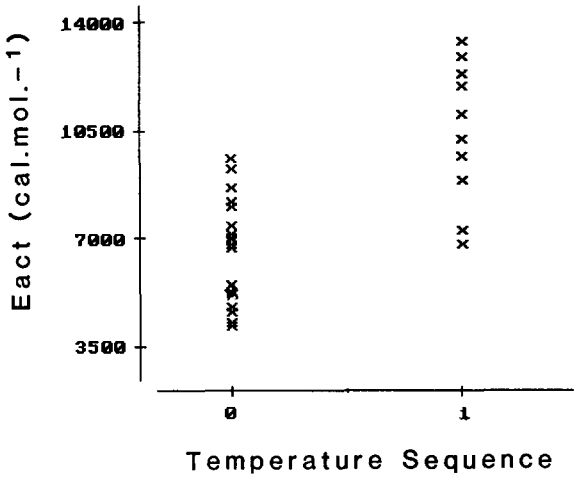

Fig. 3. Plot of E_a values for all two-temperature runs, showing the difference between those obtained when the first measurement was made at low temperature (1) and those obtained for the opposite procedure (0).

The results from temperature dependence studies are given in Fig. 3 and Table 2. The range of E_a values is 4.2–13.3 kcal mol^{-1}, with significantly higher values being obtained when the first set of measurements was at low temperature, and low E_a values for the opposite temperature order. A Mann-Whitney test of the data gave significantly different medians of 6.9 and 10.6 kcal mol^{-1} ($p < 0.01$), respectively.

The NMR study confirmed the presence of acetone within one sample of crystals of HMM and a trace of acetone within a second crystalline sample.

Discussion

The overall result of the study is that the ends of the crystals, as measured in the manner described, generally diminish at a faster rate than the sides (mean value $R_L/R_W = 1.57$). The observed changes in length and width represent the overall projected changes resulting from dissolution at a range of different crystal faces, shown

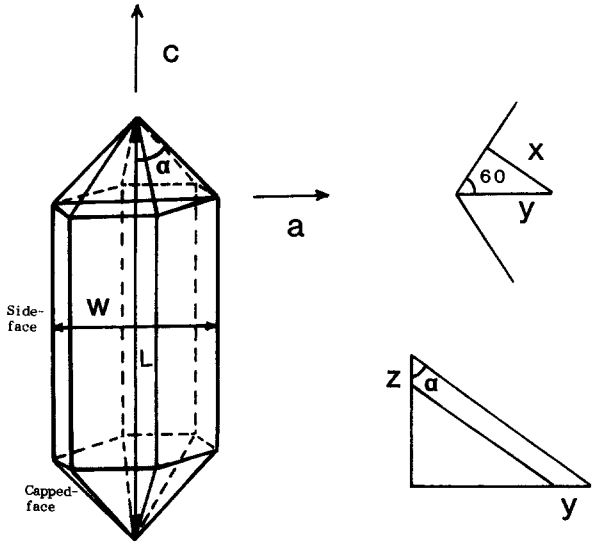

Fig. 4. Geometrical features of the dissolution of HMM crystals.

for the idealised crystal form in Fig. 4. For example, if the rate of dissolution at each of the faces parallel to the c-axis is the same at x mm min^{-1} (i.e., perpendicular to these faces) the observed change in width will be $y = c \cdot 2x/\sin 60°$ (the crystals were generally viewed perpendicular to one of the faces parallel to c). However, for the change in length the situation is more complex. The angle between faces is 109.12° in projection, leading to a relationship between y and z (Fig. 4) of $z = y/\tan 54.56°$. Consequently, assuming the rate of dissolution is the same at each face of the crystal, the observed rate of change in projected length will be smaller by a factor of 0.71. Thus, the observed average R_L/R_W ratio should be corrected by 1/0.71 to give a value of 2.2. Working backwards this would correspond to an overall average rate ratio for dissolution of 1 1 0 1, 0 1 1 1, and 1 0 1 1 class (pyramidal) faces with respect to 1 1 0 0, 0 1 1 0 and 1 0 1 0 class (prismatic) faces of the same 2.2 value.

That individual ratios vary over a considerable range ($R_L/R_W = 0.9$–2.6) is not likely to be due to inaccuracies of measurement, either due to image processing or to some effect arising from the variable thicknesses of the crystals. It has been previously noted that crystal growth rates under controlled conditions show a considerable spread (Chan et al., 1991). The same kind of spread observed in this dissolution study may reflect differences in the quality of crystals. In some of the cases a faster rate was observed for the 'interior' of the crystal (after the exterior dissolved), while for others the change was to a slower rate, indicating different states of crystallinity within the one crystal. It was the knowledge of such an effect that led to the variable temperature E_a study being carried out in both the high-to-low and low-to-high temperature sequences.

The E_a study showed that higher E_a values were obtained when the low-temperature study was done before the high-temperature one. It is possible that this arises from a general imperfection in the crystal lattice that occurs as the result of the expansion-contraction and reverse processes the crystals are subjected to. This could lead to a faster rate of dissolution than otherwise expected, for the second run of each pair. Such an effect would explain the overall trend in E_a values. An isothermal study, where the crystal was removed from the solution, as in the two-temperature studies, showed some indication of an increase in rate. However, a complicating factor is that in some cases a faster rate was observed for the inner portion of the crystal (after the exterior portion dissolved), while for others the change was to a slower rate, indicating different states of crystallinity within the one crystal. This probably contributes to the general spread of values shown in Fig. 3.

An observation that may be related to this evidence that the crystals are susceptible to thermal changes is the finding of entrapped 'bubbles' in some preparations of crystals (which have not been chosen for the dissolution measurement). The NMR study has confirmed in a sample that the small amounts of solvent (acetone) are present within air-dried crystals. What appears to happen is that the solvent becomes entrapped in hollow channels parallel to the crystal axis. In general crystals that did not appear to have these channels were selected for the dissolution studies. However, some finer channels, not obvious under microscope, could have been present. This may be related to the existence of open channels

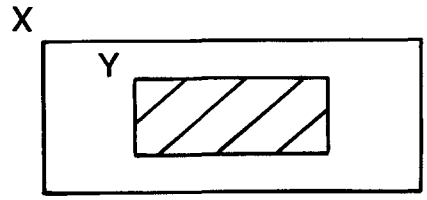

Fig. 5. Dissolution of crystal X to crystal Y, for the axial ratio to be maintained at 2.5, requires a R_L/R_W ratio of the same value.

in the crystal lattice, parallel to the *c*-axis (Bullen et al., 1972) and the basic looseness of the crystal packing. While the dimensions of the channels may not be large enough to accommodate solvent molecules (usually acetone), they could facilitate the erosion of the structure at a macroscopic level to give the hollow channels observed.

The average E_a value measured in these experiments falls between the ranges of 2.8–7.0 and 10–29 kcal mol^{-1}, regarded to be those corresponding to transport-controlled processes and surface-controlled reactions, respectively (Burt and Mitchell, 1979, 1981). Because other evidence from stirring studies indicates that diffusion is not rate determining, the results suggest a surface-controlled dissolution process.

On the other hand, the pre-exponential term, being relatively high when E_a is low, and vice versa, indicates an orientational factor, at the molecular level, is also important (and perhaps dominant) in the dissolution process. This could be related to the fact that at the molecular level, the capped faces of the crystal are smoother than the more rugged side faces (Fig. 6) (Bullen et al., 1972; Hartman and Chan, 1993). Thus, the critical factor for HMM dissolution may be the orientation of the solute and solvent molecules on the crystal surfaces. The HMM molecules at the capped faces could be more readily 'peeled away' by solvent interactions than for the side faces where the stacking is more staggered.

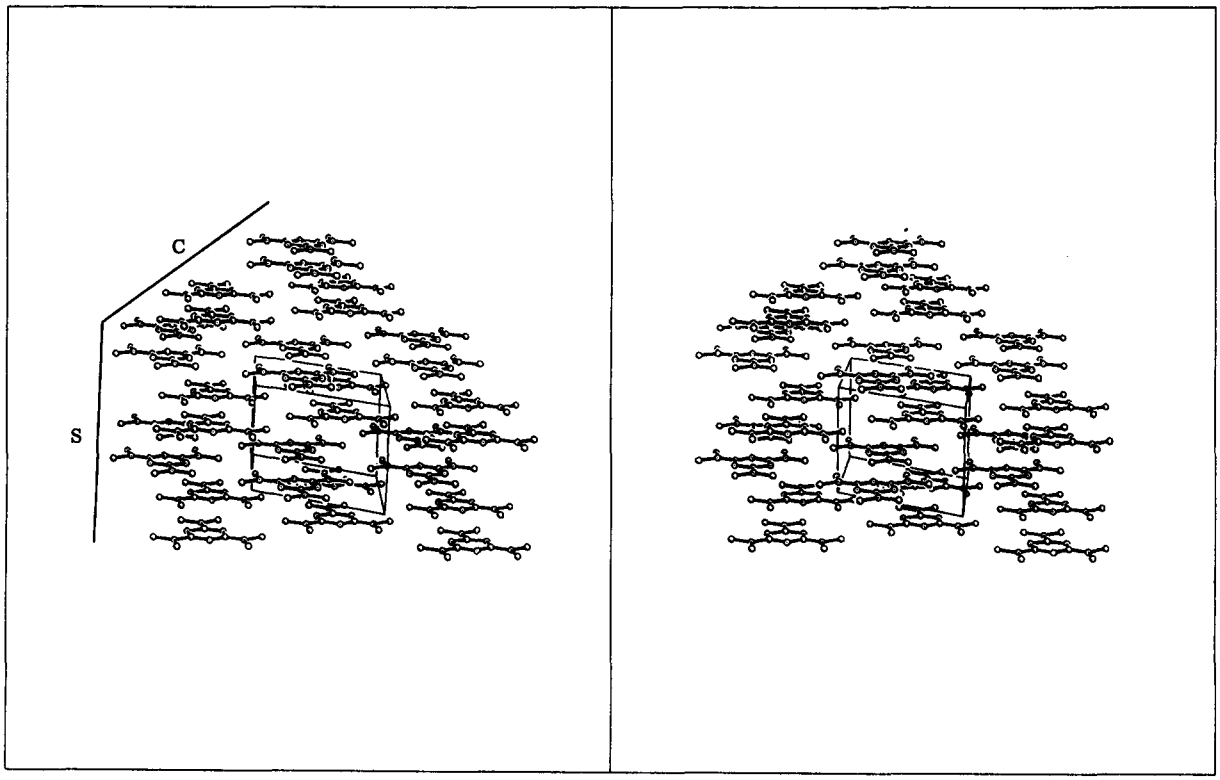

Fig. 6. Stereodiagram of the crystal packing of HMM showing the disposition of the molecules on the capped (C) and side (S) faces.

An analysis of E_a and the pre-exponential factor (A) values using all of the two-temperature R_L and R_W results as one data set gave the expressions

$$E_a(L) = -1604 + 1.17E_a(W) \quad (1)$$

and

$$A(L) = -2.3 + 1.17A(W) \quad (2)$$

at coefficient of determination R^2 (adj) ~ 0.6. These values indicate specific differences for L and W. It should be observed that the relationship between E_a(L) and E_a(W) is actually the opposite one expected for $R_L > R_W$. Hence, the critical factor controlling HMM dissolution is that of A having a higher value for L than for W. These results tend to confirm the indication that the key factor producing $R_L > R_W$ is an orientational one.

The fact that the mean slopes in Eqns 1 and 2 are identical could be fortuitous. The low values of the correlation coefficients do not warrant analysis of a possible entropy-enthalpy compensation effect (Tomlinson, 1983).

The observed (corrected) range of about 2 for R_L/R_W matches that observed for the growth of HMM in methanol and cyclohexane at various stages of crystallisation (about 1–2.4 excluding extreme initial and final values) (Chan et al., 1991). Taken together, these growth and dissolution results indicate the ratio is an inherent property of the crystals, as suggested above, and that the processes are not influenced by diffusional factors.

The results would therefore indicate that solute-solvent interactions are not responsible for the differences observed in the dissolution studies. However, this means that the significantly greater tendency to obtain needle crystals, rather than 'compact' ones, from polar solvents, must be related to a non-equilibrium factor that enhances growth anisotropy for such solvents. The 2.2 factor is significantly lower than that required to sustain the growth of needle crystals, even when the crystals nucleate as small needles. This may be appreciated by considering that for the reverse process of dissolution, for a crystal of axial ratio 10, the dissolution rate ratio would have to be maintained at that same value for the crystal to maintain its original shape (Fig. 5). Thus an amplifying non-equilibrium factor must operate in all cases of HMM needle formation in order to significantly enhance the inherent bias towards axial growth.

Intuitively, one might consider the dissolution process as the reverse of growth: solvent adsorption on certain crystal faces hinders the growth but facilitates the dissolution of those faces. But it is known that due to the different rate determining step in the two processes, crystallization and dissolution are not necessarily to be reciprocal (Mullin, 1972). In reality, it has been recently reported that solvent binding could lead to both fast growth and dissolution (Weissbuch et al., 1991). The finding was explained by a complex 'relay' mechanism. Although the explanation appears to be different, the case with HMM is similar: both growth and dissolution rate are faster along the c-axis.

One of our original aims was to investigate whether inherent features of crystal packing may, in certain cases, dominate both crystal growth and dissolution, even though the latter can be different from each other mechanistically. It may be seen from the results that the ratio of the rates of dissolution are basically independent of the solvent used and the absolute rate values. In particular changing from a polar (methanol) to a nonpolar (cyclohexane and cyclooctane – runs 10 and 12 respectively) solvent shows no major change. Similarly, varying the composition of water-methanol mixtures had no systematic effect on the results (data not shown). We therefore conclude that, unlike the growth of HMM crystals which is solvent dependent, the relative dissolution rates of HMM crystal faces were controlled by the crystal packing and not by the solvent polarity.

We hypothesise that the crystal packing features impose an inherent anisotropy, both for crystal growth and dissolution. In the case of growth, this may be amplified (via solvent interactions, crystal defects and the presence of narrow channels along the c-axis) to give the observation

of needle growth. More generally, such a built-in anisotropy may make the system much more susceptible to non-equilibrium effects than would otherwise be the case. Thus, a particularly loose kind of crystal packing may allow a much more significant role to be played by the solvent in crystal growth. Thus subtle orientational effects at the molecular level may be crucial as well as particular concentration, temperature and rate of crystallisation.

Acknowledgments

We thank Mr B.N. Tattam for determining NMR spectra and Dr E.V.A. McKee for providing the crystal packing stereodiagram (Fig. 6).

References

Aroney, M.J., Hambley, T.W., Patsalides, E., Pierens, R.K., Chan H.-K. and Gonda, I., Hexamethylmelamine: a study of solvation and crystallization. *J. Chem. Soc. Perkin II,* (1987) 1747–1752.

Bullen, G.J., Corney, D.J. and Stephens, F.S., Crystal and molecular structure of hexamethylmelamine [2,4,6-tris-(dimethylamino)-1,3,5-triazine]. *J. Chem. Soc. Perkin II,* (1972) 642–646.

Burt, H.M. and Mitchell, A.G., Dissolution anisotropy in nickel sulfate α hexahydrate crystals. *Int. J. Pharm.,* 3 (1979) 261–274.

Burt, H.M. and Mitchell, A.G., Effect of habit modification on dissolution rate. *Int. J. Pharm.,* 5 (1980) 239–251.

Burt, H.M. and Mitchell, A.G., Crystal defects and dissolution. *Int. J. Pharm.,* 9 (1981) 137–152.

Chan, H.-K. and Gonda, I., Studies of the mechanism of crystal growth of hexamethylmelamine: II. Rates of growth of the crystal faces. *J. Cryst. Growth,* 108 (1991) 751–758.

Chan, H.-K., Gonda, I. and McLachlan, A., Studies of the mechanism of crystal growth of hexamethylmelamine: I. Solute-solvent interaction. *J. Cryst. Growth,* 104 (1990) 355–365.

Chan, H.-K. and Grant, D.J.W., Influence of compaction on the intrinsic dissolution rate of modified acetaminophen and adipic acid crystals. *Int. J. Pharm.,* 57 (1989) 117–124.

Hartman, P. and Chan, H.-K., Application of the periodic bond chain (PBC) theory and attachment energy consideration to derive the crystal morphology of hexamethylmelamine. *Pharm. Res.,* (1993) in press.

Mullin, J.W., *Crystallisation,* 2nd Edn, Butterworth, London, 1972, pp. 199–200.

Tomlinson, E., Enthalpy-entropy compensation analysis of pharmaceutical, biochemical and biological systems. *Int. J. Pharm.,* 13 (1983) 115–144.

Weissbuch, I., Addadi, L., Lahav, M. and Leiserowitz, L., Molecular recognition at crystal interfaces. *Science,* 253 (1991) 637–645.